

The dielectric properties of mica paper in variable temperature and humidity

M. ASHRAF CHAUDHRY*, ANDREW K. JONSCHER

Chelsea Dielectrics Group, Chelsea College, Pulton Place, London SW6 5PR, UK

The complex capacitance of mica paper is influenced exponentially by variations in the reciprocal temperature and the relative humidity. This response is dominated by the peripheral line contacts between mica flakes, rather than by the surface impedance of the mica flakes between these contacts. The resulting complex capacitance shows low-frequency dispersion at high humidities and high temperatures, and a less dispersive power law at high frequencies, low humidities and low temperatures. The physical significance of these results is discussed.

1. Introduction

"Mica paper" is a paper-like material made of finely flaked mica pressed together into cohesive sheets held together by van der Waals forces, without the intervention of any binders. The material is, therefore, pure mica, without any cellulose or other organic content and the only connection with ordinary paper is the similarity of the end product and the method of production [1]. Some measurements of the dielectric properties of mica paper with temperature as a parameter was reported by Aleksandrov *et al.* [2] who found a decrease of direct current (d.c.) conduction with rising temperature, presumably as a result of the loss of residual humidity. No systematic studies of the effects of humidity on the dielectric properties of mica paper appear to have been published, and yet one would expect humidity to be an important parameter both from the fundamental standpoint and in practical applications. We have therefore undertaken a systematic study of the effect of humidity on the dielectric response of mica paper, while the complementary study of the effect of temperature appeared highly desirable in view of the availability of our wide frequency range, stretching down to very low frequencies which had not previously been investigated. Moreover, we have applied to the analysis of our experimental data our general method of approach based on the

concept of the "universal" dielectric response of solids [3] and in particular on the low-frequency dispersion (LFD) [3-5] which has a dominant influence at low frequencies and which is often mistaken for d.c. conduction. This approach has led to a better understanding of the processes involved. The present work is complementary to the study of surface conduction on mica and the role of contacts in that context [6].

The effects of humidity on the dielectric properties of mica paper resemble those on other surface-conducting granular systems, e.g. sand [7] and also on many other water-containing materials such as zeolites [8] and biological systems [9]. The significance of the response of mica paper lies in the predominance of surface conduction and in the fact that in the present instance we are dealing with fine point contacts between mica flakes touching under the action of the weak cohesive forces, with the external metal contacts representing only a small effect at the end of a series of many mica-mica contacts. To that extent, therefore, the study of mica paper relates to a system in which metallic contacts play a relatively insignificant role.

2. Experimental details

Samples of mica paper for the present investigation were cut from a sheet in pieces of $20 \times 20 \text{ mm}^2$. Three types of electrode were

*Present address: Department of Physics, University of Karachi, Karachi, Pakistan.

used: copper foils pressed against the mica paper on either side; evaporated aluminium electrodes of 10 mm diameter with copper foils pressed against them; or evaporated aluminium electrodes with silver dag painted over them and attaching fine wires.

Samples were held in desiccators with saturated salt solutions providing standard relative humidity (RH) atmospheres [10, 11], with a period of three days being left before the start of measurements to allow a state of equilibrium to be reached with the ambient. This period was found empirically to be sufficient to reach steady dielectric readings. All humidity runs were taken in ascending order of RH beginning with the samples in the "dry" state (24 h in a vacuum of 10^{-3} Pa).

For measurements in variable temperatures the samples were fitted either with evaporated aluminium electrodes as described above or, for the higher temperature range, platinum foil electrodes were pressed against the mica paper. The sample holder consisted of a silica cylinder with two silica tubes carrying platinum wires terminated at the bottom with platinum sheet electrodes and shielded by stainless steel tubes. A spring-loaded central rod provided pressure to hold the mica paper sample at the bottom of the holder between the electrodes. Evaporated aluminium was capable of being used up to 910 K, platinum up to 1006 K. The sample holder was placed in a vertical furnace controlled by a Eurotherm controller, with temperature measurement by a chromel–alumel thermocouple.

Temperature runs were made separately for rising and falling temperatures, the principal difference being that in the latter case the sample may be presumed to be dry, according to the highest temperature of the given run, while in the former some moisture may be expelled during heating. These separate runs will be denoted by the symbols $T\uparrow$ and $T\downarrow$, respectively.

Electrical measurements were made on a Solartron frequency response analyser (FRA) specially adapted for this purpose by the Chelsea Dielectrics Group [12] and operating in the range 10^{-2} to 10^4 Hz. The results are presented as logarithmic plots of the frequency dependence of the real and imaginary components of the complex capacitance:

$$\begin{aligned}\tilde{C}(\omega) &= C'(\omega) - iC''(\omega) \\ &= C'(\omega) - iG(\omega)/\omega\end{aligned}\quad (1)$$

where $G(\omega)$ is the frequency-dependent alternating current conductance. In some cases it is preferable to plot the frequency-dependent equivalent dielectric susceptibility [3]:

$$\begin{aligned}\hat{C}(\omega) &= \hat{C}'(\omega) - i\hat{C}''(\omega) \\ &= C(\omega) - C_\infty + iG_0/\omega\end{aligned}\quad (2)$$

which is the complex capacitance corrected for the "infinitely high frequency" capacitance C_∞ and for the d.c. conductance G_0 . The advantage of this representation is that $\hat{C}'(\omega)$ and $\hat{C}''(\omega)$ are directly Kramers–Kronig compatible, and in the majority of cases presented in this work they both follow the universal dielectric law [3]

$$\hat{C}'(\omega) = \tan(n\pi/2)\hat{C}''(\omega) \propto \omega^{n-1} \quad (3)$$

where the exponent takes values in the range $0 < n < 1$. Normal low-loss dielectrics show n values close to unity; LFD corresponds to $n \rightarrow 0$. In the $\log \hat{C}(\omega) - \log \omega$ representation $\hat{C}'(\omega)$ and $\hat{C}''(\omega)$ are therefore two parallel straight lines of slope $(n - 1)$ and with a ratio given by Equation 3.

Some of our data are presented in normalized form, either with respect to humidity or to temperature [3] in order to bring out the general form of the respective relationships, resulting in a much wider frequency range and also providing a direct measure of the dependence of the frequency shift on temperature and on humidity, respectively.

3. Results

3.1. Temperature dependence

The response of Sample 16 with evaporated aluminium electrodes is shown in Fig. 1 for $T\uparrow$ and in Fig. 2 for $T\downarrow$. In both cases $C'(\omega)$ and $C''(\omega)$ are being presented and normalized, i.e. no subtraction is made of C_∞ and G_0 . At 360 and 445 K the loss is relatively low, $\tan \delta = C''/C'$ being 3×10^{-3} at the highest frequencies, which is not as low as in crystalline mica normal to the cleavage planes but is common for mica paper. As the temperature reaches 600 K, LFD sets in visibly and increases continuously to the highest temperature of 914 K which is dictated by the endurance of the aluminium contacts. The normalization of these results in Figs. 1c and 2c

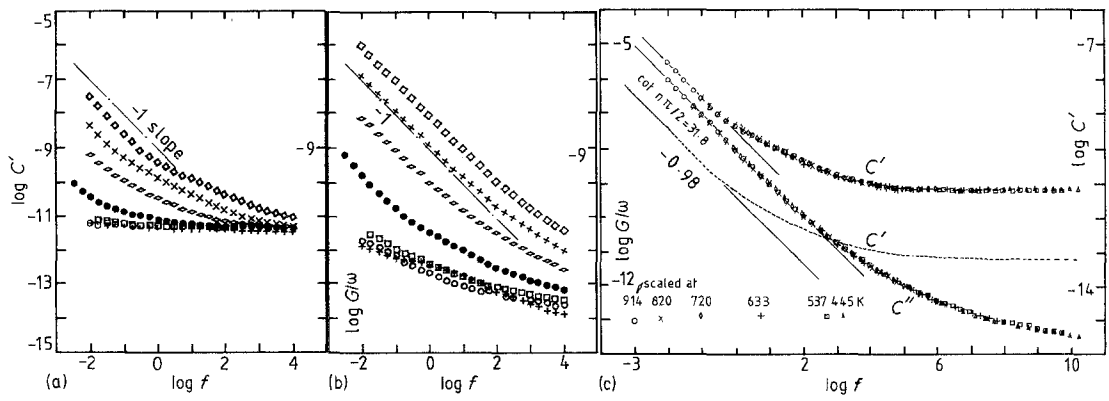


Figure 1 The temperature dependence of the frequency-dependent complex capacitance $\tilde{C}'(\omega)$ and $\tilde{C}''(\omega)$ for mica paper Sample 16 with evaporated aluminium electrodes, for $T \uparrow$. (a) and (b) show two separate families of curves, (c) gives the normalization with the locus of a reference point, with the real part raised by two decades for clarity, its relative position to the imaginary part being shown by the dotted line. Units of capacitance F, frequency Hz. Temperatures (K): + 360, O 445, □ 537, ● 633, ∇ 727, × 820, ◇ 914.

shows a limiting slope of practically -1 at low frequencies, but the relative positions of the real and imaginary plots suggest a value of $(1 - n) = 0.98$. The interesting point is that the $C'(\omega)$ data deviate from the LFD trend much sooner than the $C''(\omega)$ data, showing that an additional loss process is buried under the LFD loss. An interesting detail is that in the $T \downarrow$ results the 360 K data fall above the 445 K data except at the lowest frequencies, falling rapidly at higher frequencies. A similar situation is found on the rising temperature runs, and both may be due to the presence of moisture at the lower temperatures compared with the higher temperatures. This means that normalization is difficult in this temperature range. Apart from this, the C' and C'' data are very similar in their general appearance, while the respective activation energies will be described later. It is

worth noting that there is no visible sign of d.c. conductivity even at the highest temperatures, as would be evident by an abnormal rise of the $C''(\omega)/C'(\omega)$ ratio which is not apparent here.

The corresponding results for platinum contacts are shown in Figs. 3 and 4, and a similar phenomenon of abnormal loss response between 360 and 445 K is seen for decreasing temperatures as in Fig. 2.

It is noteworthy that with both aluminium and platinum contacts the decreasing-temperature results lie consistently above those for increasing temperatures. The reason for this is not very clear, since it cannot be due to residual moisture, which would have been higher in rising temperatures. Both contacts likewise show a trend with $n = 1/2$ at high frequencies and low temperatures, for which $\hat{C}' = \hat{C}''(\omega)$ and which is classically associated with diffusive

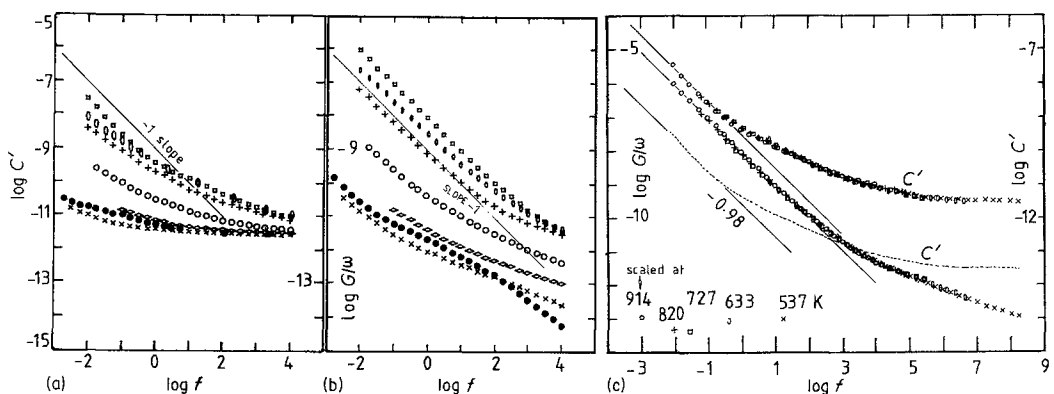


Figure 2 Similar data as in Fig. 1 but for $T \downarrow$. Temperatures (K): □ 914, O 820, + 727, O 633, ◇ 537, × 445, ● 360.

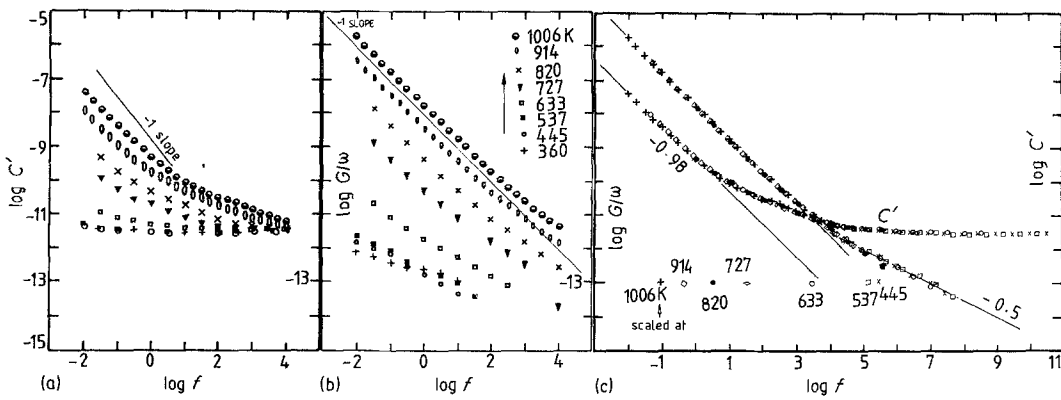


Figure 3 The dielectric response of mica paper Sample 18 with platinum pressure contacts for $T\uparrow$. In the normalized plot the real and imaginary components are shown on the same scales. Temperatures are indicated on graph.

processes [3], although it is worth pointing out that this interpretation is not necessarily unique and this may be simply a special case of the universal law, not connected with diffusion.

The activation energies may be obtained from the frequency shift of the representative points in the normalization plots and they are shown in Fig. 5 for the data shown in Figs. 1 to 4. The values obtained, with the exception of the lowest temperature points, are listed in Table I. We have already noted that the higher values for increasing temperatures may be related to the fact that water is being driven out in this process.

We note that the LFD response did not change on the application of a 10 V bias on top of the 1 V rms alternating signal, and this signifies that the response is linear in the applied bias. This result is not surprising in view of the fact that mica paper samples have many contacts in series, and therefore there is little chance

of developing a significant voltage across any one of them.

3.2. Humidity dependence

We begin the presentation with a sample of mica paper with evaporated aluminium and copper foil backing as contacts. A family of curves of $C'(\omega)$ and $C''(\omega)$ is shown in Fig. 6, including the response of the sample placed in a vacuum. It may be noted that already with 23% RH there is a visible dispersion of C' , and C'' has increased by nearly two orders of magnitude. Subsequent increases of RH bring about relatively smaller rises and there is a tendency to saturation at the highest humidities. The normalization in Fig. 6c shows clearly a limiting slope of -0.8 with K-K-compatible $C'(\omega)$ and $C''(\omega)$. There is a pronounced structure in both components at frequencies in excess of the region in which LFD is dominating; this

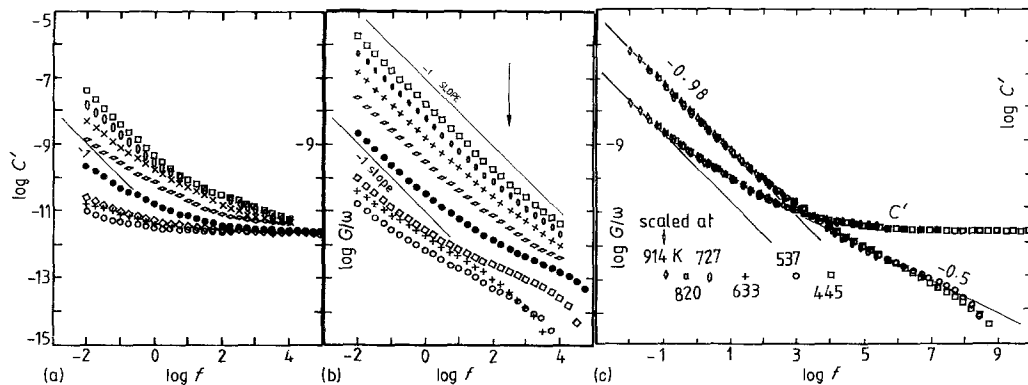


Figure 4 Similar data as in Fig. 3 but for $T\downarrow$. Temperatures (K): \square 1006, \circ 914, \times 820, \diamond 727, \bullet 633, \diamond 537, \circ 445, $+$ 360.

TABLE I Activation energies for different contacts

	Activation energy (eV)	
	Aluminium	Platinum
$T\downarrow$	1.1	1.1
$T\uparrow$	1.6	1.4

behaviour resembles that seen at intermediate temperatures. The limiting slope of loss at high frequencies and low humidities is -0.33 , significantly less than the 0.5 slope in temperature runs.

Very similar data were obtained for a sample with copper foil contacts, which we show only in normalized form (Fig. 7). Here a difficulty presents itself in the normalization process. If "best fit" of data is attempted to produce the smoothest form of master curve for all humidities, then the locus of the characteristic point rises towards higher humidities, as shown in Fig. 7a, which implies that the amplitude of the more humid response *decreases*. Physically this is not a very plausible conclusion, and we therefore present in Fig. 7b an alternative normalization where we have retained the assumption of a constant amplitude with increasing humidity. The low-frequency and high-frequency limits of the normalized master curve are naturally unchanged compared with Fig. 7a, but the middle part shows an evident misfit. There is nothing wrong in principle with this type of response, since all that it implies is that the exponent n in the power law [3] is changing with RH without going smoothly from one value to another. We believe, therefore, that the nor-

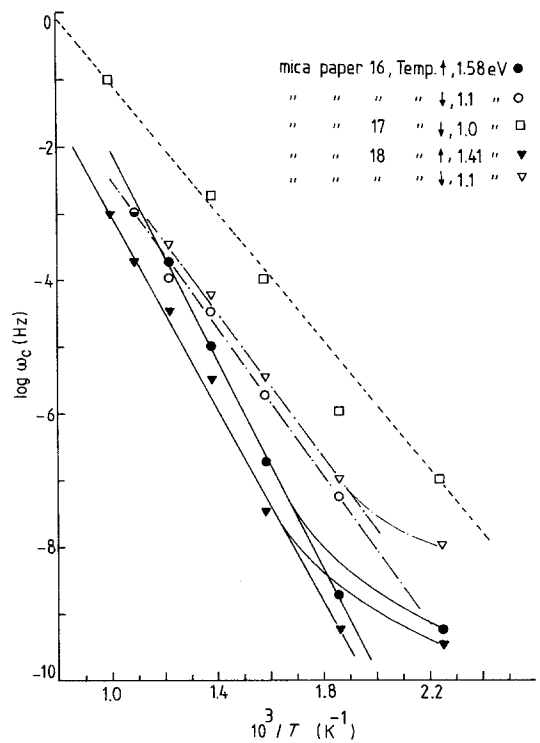


Figure 5 Activation plots for the samples shown in Figs. 1 to 4, with one more sample added, with the activation energies shown in the inset.

malization in Fig. 7b corresponds better to physical reality than the apparently more "regular" shape in Fig. 7a.

It should be noted that the high-frequency response in Fig. 7 has the same slope as the corresponding part in Fig. 6, while the low-frequency LFD shows a slightly different value.

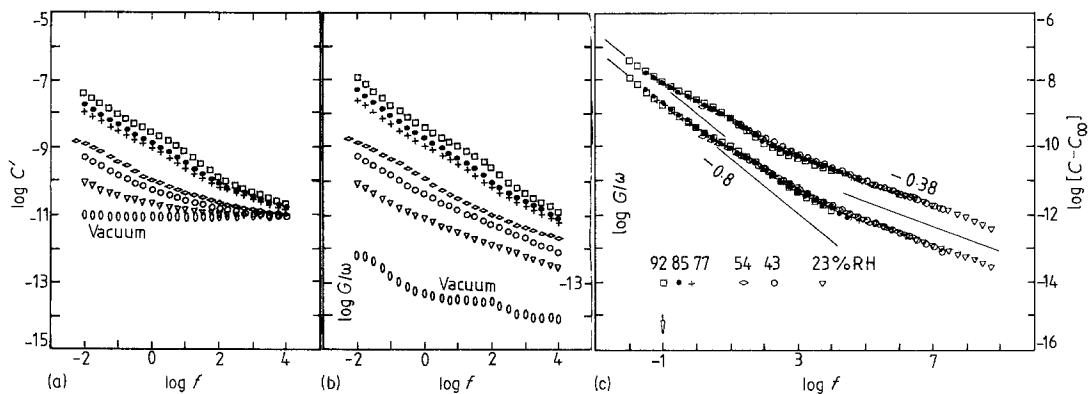


Figure 6 Humidity dependence of the complex capacitance for Sample 8 with evaporated aluminium contacts capped by copper foil. The normalization plot refers to the susceptibility $\tilde{C}(\omega)$. The vacuum data were not normalized with the rest, since they did not fit into the general pattern. The locus of a reference point is shown. Units of capacitance F, frequency Hz. RH (%): ∇ 23, \circ 43, \diamond 54, $+$ 77, \bullet 85, \square 92.

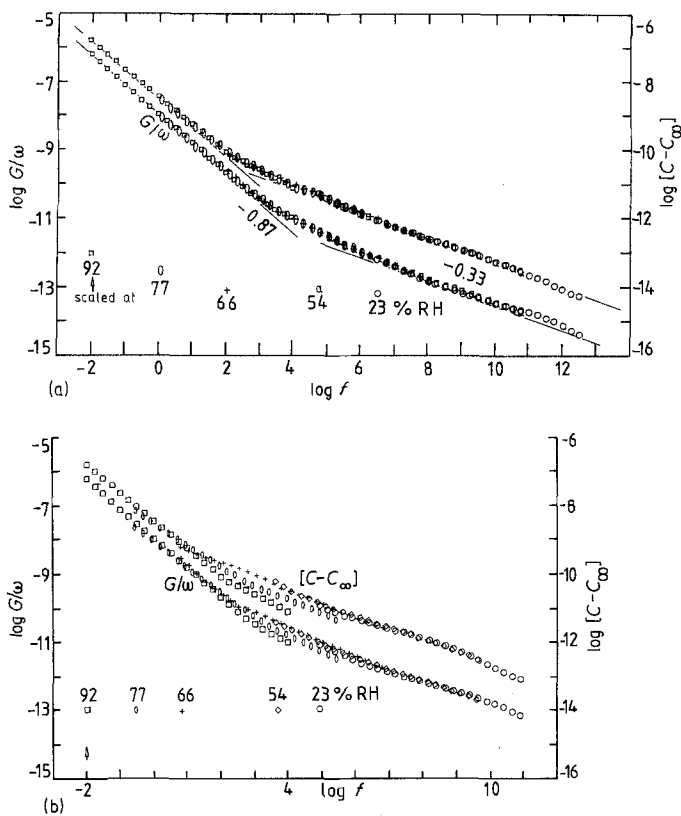


Figure 7 The normalized data for humidity dependence of Sample 12 with copper foil contacts, plotted as the susceptibility $\tilde{C}(\omega)$. The two graphs show slightly different methods of normalization, (a) giving the "best fit" for which the reference points rise, indicating a decrease of amplitude with rising humidity, which we regard as physically implausible. Diagram (b) shows the normalization with a constant amplitude, for which the resulting plot is not as well-fitting as in (a) but which may be physically more plausible, indicating that the middle portion corresponds to a different form of humidity dependence.

Finally, Fig. 8 gives a normalized response of a sample with evaporated aluminium contacts covered with silver paint, normalized according to the same principle as Fig. 7b, i.e. on the assumption of a constant amplitude of response with RH. The overall shape of the normalized curve is closely similar to that in Fig. 7b except that the LFD region covers a wider range of frequencies.

The "activation" plots of the frequency shift under normalization with RH as a variable parameter are constructed in the same way as the thermal activation energy plots and are shown in Fig. 9. They form substantially straight lines of $\log \omega_c$ against linear RH, but the more significant quantity would be the dependence on surface concentration of water molecules which is not known. Assuming, however, that barring some saturation effects at more than a monolayer coverage, the surface concentration is some moderately linear function of RH, then the conclusion from Fig. 9 is that the frequency shift has some form of *exponential* dependence on the surface concentration of water molecules.

This somewhat surprising result is in line with earlier findings for the surface conductance of

humid sand grains [3, 7] and also for "bulk conduction" in zeolites in which the effective transport process is migration on internal cavities in the material [8].

4. Discussion of results

The general conclusions which may be drawn from the experimental results of measurements of the effects of both temperature and humidity on the dielectric properties of mica paper are as follows:

(a) The similarity of the spectral shape of the normalized response suggests that the two influences, temperature and humidity, are physically closely related. The differences in the power-law exponents are easily accounted for in terms of the very different temperature regimes in which the two sets of measurements are being made.

(b) There are two principal ranges of power-law dispersion, one LFD at high humidities and high temperatures, the other less dispersive at high frequencies with low humidities and low temperatures. These two clearly defined regions are joined by an intermediate range in which there is evidence of a secondary loss peak

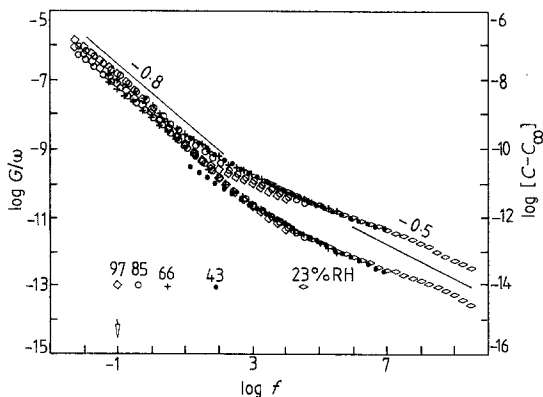


Figure 8 The normalized $\hat{C}(\omega)$ response of a sample of mica paper with evaporated aluminium contacts covered with silver paint, normalized according to the same convention as in Fig. 7b, the real part being raised by one decade for clarity.

process at frequencies just above the LFD range. There is also incompatibility of the RH results with continuous normalization, suggesting that the exponent of the power law changes with RH without going smoothly from one value to another.

(c) The exponents in the two regions and for the temperature and RH runs may be expressed numerically as shown in Table II.

(d) The nature of the metallic contacts does not make a first-order difference to the behaviour of the response either with temperature or with RH.

(e) The dependence of the frequency shift in normalization on $1/T$ and on RH appears to be exponential, in the former case producing higher activation energies for $T \uparrow$ than for $T \downarrow$, in agreement with the notion that water has to be expelled in the former case. The significance of

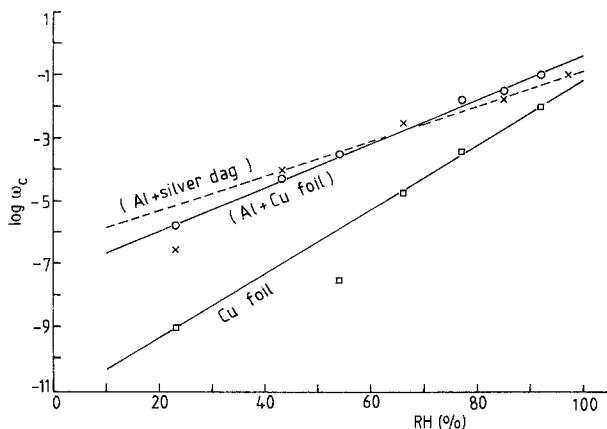


Figure 9 The "activation" plots with respect to changing humidity of the displacement of the reference points along the frequency axis. Almost linear dependence of the logarithm of frequency displacement on relative humidity is seen.

TABLE II Values of the power-law exponent n

	Variable	
	Temperature	RH
Low frequency	0.02	0.2
High frequency	0.55 to 0.5	0.65 to 0.7

these results is that in both cases one is accelerating exponentially the probabilities of hopping transitions, in the case of temperature due to the increasing thermal energy available, in the case of humidity by providing additional sites for percolation of molecules. The important conclusion here is that humidity does not influence proportionally the *density* of available carriers, but makes their transitions exponentially more probable.

In the interpretation of these results we have to bear in mind the nature of the contacts and of the surface conduction processes in mica paper. The contacts are definitely of nearly a point nature, being due mainly to the weak cohesive forces between the individual flakes which are not otherwise bonded in any way. This very small contact acts essentially through its periphery, since the element of bulk conduction may be assumed to be negligibly small in the case of RH variation at room temperature. The similarity of response with variable temperature suggests then that the same is also the case there.

5. Contacts and spreading resistance

The situation near one of these point contacts may be envisaged as shown schematically in Fig. 10. The spreading impedance on the surface of the grain will be denoted by Z_s and the contact

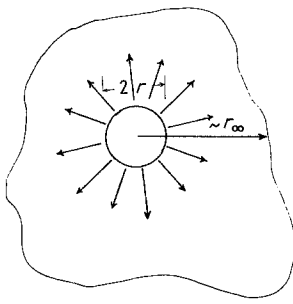


Figure 10 The spreading resistance arising from contacts between mica flakes. The actual contact is shown as a circle of radius r which is assumed to be much smaller than the dimensions of the flake represented by r_∞ , so that current flow along the surface is radial.

impedance itself by Z_c , and we envisage them being in series. We refer specifically to impedances and not simply resistances, since both of these are likely to be frequency-dependent dispersive processes; this is certainly so in the case of the contact impedance [6].

The magnitudes of these impedances depend on the diameter $2r$ of the contact itself. In the case of Z_c we may assume that the impedance is proportional to $1/r$, i.e. inversely proportional to the periphery of the contact. The spreading impedance on a sheet conductor is easily shown to be proportional to the logarithm of r_∞/r , where r_∞ stands for some "infinitely large" radius. We therefore have the two contributions as shown schematically in Fig. 11 and we note that the ratio r_∞/r is likely to be large. The proportionality factors in the impedances Z_s and Z_c are both functions of the relative humidity, although we do not know exactly what these functional relations are. There is no doubt, however, that both are decreasing with increasing humidity and vice versa. The conclusion is that the dominant effect is very likely that of the contact impedance, and the spreading impedance is insignificant.

We have assumed that the contacts behave like *peripheral line* contacts to a conducting *surface sheet*. Corresponding measurements on evaporated and painted metallic contacts to single-crystal mica have shown their complicated dispersive character [6] with, in particular, a region of strong dispersion at relatively high frequencies and with a barrier capacitance dominating the low-frequency behaviour. The very different appearance of our mica paper contacts may be understood in terms of the fact that they

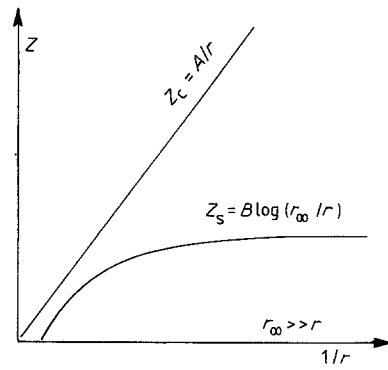


Figure 11 A plot of the magnitude of the contact impedance $Z_c \propto 1/r$ and of the spreading impedance $Z_s \propto \log(r_\infty/r)$ against $1/r$, showing that the contact impedance is likely to dominate at large values of r_∞/r .

are mica-mica contacts and not metal-mica as in [6].

6. Conclusions

Our impedance measurements on mica paper as a function of relative humidity and of temperature have shown that both these influences have rather similar effects on the frequency dependence of what is believed to be predominantly the contact impedance. There are two dominant dispersion regions which differ by their values of the power-law exponents, the more dispersive one of which may be associated with the dissociation/association of carriers at the contact interface with the surface of the mica. The fact that humidity and reciprocal temperature both influence exponentially the frequency shift in the respective normalizations throws interesting light on the nature of the humidity effect.

The mica-mica contacts which dominate the response of mica paper differ in an important respect from the metal-mica contacts, but their understanding is not perfect as yet.

Acknowledgements

One of us (M.A.C.) is indebted to the Government of Pakistan for a bursary and to the University of Karachi for study leave.

References

1. R. J. KETTERER, *Insulation* **10** (1964) p. 24.
2. E. E. ALEKSANDROV, A. I. PETRASHKO and V. A. TALGKOV, *Elektrotechnika* **50** (6) (1979) 27.
3. A. K. JONSCHER, "Dielectric Relaxation in Solids" (Chelsea Dielectrics Press, London, 1983).
4. *Idem*, *Phil. Mag.* **B38** (1978) 587.

5. *Idem*, Conference on electrical Insulation and Dielectric Phenomena (IEEE Insulation Society Publication, 1983) p. 479.
6. A. K. JONSCHER, M. A. CHAUDHRY and T. C. GOEL, *Trans IEEE-EI*, in press.
7. M. SHAHIDI, PhD thesis, University of London (1980).
8. M. A. CHAUDHRY, A. HAIDAR and A. K. JONSCHER, IEE Conference Publication No.239, DMMA (1984) p. 49.
9. F. X. HART, IEEE Conference on Electrical Insulation and Dielectric Phenomena (IEEE Insulation Society Publication, 1983) p. 391.
10. F. E. M. O'BRIEN, *J. Sci. Inst.* **25** (1948) 73.
11. G. W. C. KAYE and T. H. LABY, "Tables of Physical and chemical Constants" (Longman, London 1978) p. 28.
12. J. PUGH, IEE Conference Publication No. 239, DMMA (1984) p. 147.

*Received 18 October
and accepted 6 November 1984*